# Characterization of brivanib therapy response in hepatocellular carcinoma xenografts using $^{1}$H HR-MAS spectroscopy and histopathology

JEHOON YANG[1,3], KYOUNG DOO SONG[2], JAE-HUN KIM[2], GEUN-HO IM[4], SEULGI YOON[3], MISUN NAMGUNG[4], JUNG-HYUN HWANG[5], JUNG HEE LEE[2] and DONGIL CHOI[2]

[1]Department of Medical Science, Sungkyunkwan University School of Medicine; [2]Department of Radiology, Samsung Medical Center, Sungkyunkwan University School of Medicine; [3]Laboratory Animal Research Center, and [4]Center for Molecular and Cellular Imaging, Samsung Biomedical Research Institute, Suwon; [5]Department of Chemistry, Hankook University of Foreign Studies, Seoul, Republic of Korea

Received April 15, 2013; Accepted August 21, 2013

DOI: 10.3892/mmr.2013.1690

**Abstract.** Angiogenesis inhibition is an attractive therapeutic strategy in the management of solid tumors. Vascular endothelial growth factor (VEGF) and fibroblast growth factor (FGF) are key factors in growth and neovascularization of hepatocellular carcinoma (HCC). Brivanib is a novel, orally available dual tyrosine kinase inhibitor that selectively targets the key angiogenesis receptors VEGF-R2, FGF-R1 and FGF-R2. Recently, high-resolution magic angle spinning magnetic resonance spectroscopy (HR-MAS MRS) has provided the opportunity to investigate more detailed metabolic profiles from intact tissue specimens that are correlated with histopathology and is thus, a promising tool for monitoring changes induced by treatment. In the present study, $^{1}$H HR-MAS MRS and immunohistochemistry were used to investigate the antitumor efficacy of brivanib in HCC xenograft models. Tumor growth was significantly suppressed in brivanib-treated mice compared with the controls and treatment was associated with the inhibition of angiogenesis, increased apoptosis and inhibition of cell proliferation. Furthermore, HR-MAS techniques showed altered metabolic profiles between the two groups. HR-MAS spectra demonstrated a significant decrease in choline metabolite levels in the treated groups, concurrent with decreased cell proliferation and increased apoptosis. The results showed that $^{1}$H HR-MAS MRS provides quantitative metabolite information that may be used to analyze the efficacy of brivanib treatment in Hep3B tumor xenografts. Thus, the HR-MAS MRS technique may be a complementary method to support histopathological results and increase its potential for use in the clinic.

*Correspondence to:* Professor Dongil Choi, Department of Radiology, Samsung Medical Center, Sungkyunkwan University School of Medicine, 50 Ilwon-dong, Gangnam-gu, Seoul 135-710, Republic of Korea
E-mail: dismc.choi@samsung.com

*Key words:* angiogenesis, brivanib, high-resolution magic angle spinning magnetic resonance spectroscopy, vascular endothelial growth factor, hepatocellular carcinoma

## Introduction

Angiogenesis, the multistep process by which novel blood vessels develop from existing microvasculature in a variety of physiological states, is an essential component in solid tumor growth, invasion and metastatic pathways (1). As tumor angiogenesis is a promising target for the development of novel anticancer therapies, >12 endogenous proteins that act as activators of tumor angiogenesis have been identified (2). It is well known that tumor-induced angiogenesis is regulated by vascular endothelial growth factor (VEGF) and several other cytokines, such as platelet-derived growth factor (PDGF) and fibroblast growth factor (FGF), which are secreted by tumor cells. Among them, VEGF and its corresponding tyrosine kinase receptors, which specifically regulate endothelial proliferation, permeability and survival, are known to be part of the most important signaling pathway in physiological and pathological angiogenesis. The VEGF signaling pathway is activated by the ligand-induced phosphorylation of VEGF receptors. Blocking VEGFR phosphorylation using a kinase inhibitor is expected to disrupt VEGF signaling pathways, resulting in changes in tumor vasculature characteristics and growth. Therefore, the blockade of this antiangiogenic mechanism may provide a useful therapeutic strategy (3,4). Basic FGF (bFGF) is also a potent angiogenic factor. bFGF has been shown to be a key regulator of numerous physiological processes in adult organisms and is also involved in tumoral angiogenesis. bFGF stimulates the release and activity of collagenase, protease and integrins on the extracellular membrane to form nascent microvascular networks. Furthermore, bFGF has been shown to synergistically promote VEGF-mediated tumor development and angiogenesis in mouse models, suggesting that dual inhibition of VEGFR and FGFR pathways is an attractive therapeutic approach (5,6). A number of

pharmacological antiangiogenic agents have been investigated in clinical trials. Bevacizumab, a humanized anti-VEGF-A monoclonal antibody, showed clinical benefit in patients with metastatic colorectal cancer and was approved by the USA Food and Drug Administration (FDA) in 2004 (7). More recently, sorafenib, an inhibitor of multiple kinases, including VEGFR, PDGF receptor, c-kit, raf and flt-3, showed benefits in patients with advanced hepatocellular carcinoma (HCC) and was also approved for use in HCC by the USA FDA in 2007 (8). These achievements have validated the hypothesis that inhibition of angiogenesis may be a strategy for cancer treatment.

Brivanib (BMS-582664; Bristol-Myers Squibb, New York, NY, USA), a dual tyrosine kinase inhibitor with selectivity against the key angiogenesis receptors VEGF-R2, FGF-R1 and FGF-R2, is currently under development for the treatment of cancer as a single agent as well as in combination with other cancer treatment modalities. This compound is an orally available investigational small molecule and predominantly undergoes oxidative hepatic metabolism by CYP3A4 and CYP1A2 equally. The peak concentration of brivanib in the plasma is reached after 1-2 h and it is primarily eliminated in the feces (9). In several tumor xenograft models, brivanib has shown significant tumor growth inhibition when administered orally over multiple dose levels, suggesting that it is effective in the treatment of HCC (10,11).

High-resolution magic angle spinning magnetic resonance spectroscopy (HR-MAS MRS), an *ex vivo* MRS technique introduced in 1997, has recently become important for analyzing metabolic profiles from intact tissue specimens that contain information on the physiological and pathological status of the tumor. Comparisons of HR-MAS MRS using small biopsies and conventional high-resolution $^{1}$H MRS using perchloric acid extracts have provided similar sensitivity and resolution (12). Due to its closer and realistic insights, the application of the HR-MAS MRS technique has increasingly been utilized for the analysis of intact tissues, predominantly in cancer research (13). Previous studies have shown that the quantification of tumor metabolic changes with $^{1}$H HR-MAS MRS, in conjunction with subsequent histopathology of the same tumor specimen, supplements histopathological examination and improves the accuracy in the diagnosis, characterization, and evaluation of tumor progression in different tumors, including prostate (14,15), brain (16), lung (17), breast (12), hepatic (10) and cervical tumors (18). Therefore, this study was designed to investigate whether $^{1}$H HR-MAS MRS supplements histopathological examination and provides quantitative metabolite information for the analysis of the efficacy of brivanib treatment in Hep3B tumor xenografts. Proliferation, apoptosis and microvasculature, determined by histopathology, were also used as measures for the effect of brivanib treatment.

## Materials and methods

*Tumor cell line*. The Hep3B human hepatocellular carcinoma cell line was purchased from the Korean Cell Line Bank (Seoul, Korea) and cultured in minimal essential medium supplemented with 10% fetal bovine serum, 1% ampicillin and 1% streptomycin. Cells were cultured at 37˚C in a humidified incubator containing 5% $CO_2$ and were passaged twice a week at a split ratio of 1:3. All the experiments were conducted with 70-80% confluent cultures.

*Xenograft tumor model and brivanib treatment*. Male athymic BALB/c nu/nu mice (age, 7 weeks) were purchased from Orient Bio (Seoul, Korea) and maintained in a specific pathogen-free mouse colony at the Laboratory Animal Research Center, Samsung Biomedical Research Institute (SBRI; Seoul, Korea). The mice were maintained in accordance with guidelines of the Association for Assessment and Accreditation of Laboratory Animal Care International (Guide for the Care and Use of Laboratory Animals), and all murine studies were reviewed and approved by the Institutional Animal Care and Use Committee of SBRI (approved proposal #S-B1-002). Ectopic xenograft tumors were established by subcutaneous injection of $5x10^{6}$ Hep3B cells in a total volume of 0.1 ml serum-free medium into the right thigh under anesthetic using 1.5% isoflurane, 70% $N_2O$ and 30% $O_2$. Tumor volume was estimated using caliper measurements and calculated using the equation $v = \pi/6 \times a \times b \times c$, where a, b and c are caliper measurements of tumor length, width and depth, respectively. Tumor development was followed in individual animals every other day by sequential caliper measurements. When the tumor volume reached ~50-70 $mm^3$, the mice were randomized into two groups and brivanib therapy was initiated. Brivanib was obtained from Bristol-Myers Squibb and prepared as a suspension in vehicle (70% polyethylene glycol 400) for oral administration to xenografted tumor-bearing mice. In the treated group (n=8), mice were treated daily with oral administration of brivanib at 90 mg/kg body weight for 18 days. In the control group (n=7), mice were treated daily with an equivalent volume of vehicle. On day 18 following treatment, the mice were sacrificed and the tumors were removed. The tumor tissues were sharply excised and fixed in 10% neutral-buffered formalin for histological analysis or snap-frozen in liquid nitrogen prior to storage at -80˚C for immediate *ex vivo* HR-MAS MRS data acquisition.

*Immunohistochemistry and terminal deoxynucleotidyl transferase dUTP nick end-labeling (TUNEL) assay*. Formalin-fixed, paraffin-embedded samples were sliced into 4-$\mu$m sections, deparaffinized in xylene, rehydrated in graded alcohol and transferred to 0.01 M phosphate-buffered saline (PBS, pH 7.4). For immunohistochemical localization of Ki-67 (a marker for cell proliferation) and CD31 (a marker for tumor microvascularity) in the sections, heat-induced epitope retrieval was performed with citrate buffer (pH 6.0; Dako, Carpinteria, CA, USA) for 5 min at 121˚C to identify hidden antigen epitopes and the sections were then cooled to room temperature. Endogenous peroxidase was blocked by incubating slides with 3% hydrogen peroxide in PBS for 30 min at room temperature. Subsequent to washing in PBS, sections were treated with serum-free blocking solution (Dako) for 20 min at room temperature to block non-specific binding. Subsequently, the sections were incubated with Ki-67 rabbit polyclonal antibody (1/200; Dako) or CD31 mouse monoclonal antibody (1/150; BD Biosciences, Erembodegem, Belgium) for 60 min at room temperature. The sections were then washed in PBS and incubated for 30 min at room temperature with

horseradish peroxidase-labeled polymer conjugated secondary antibodies against rabbit IgG (Dako). The color reaction was developed using the ready-to-use DAB (3,3'-diaminobenzidine) substrate-chromogen solution (Dako) for 5 min and then washed with distilled water. Sections were lightly counterstained with Mayer's hematoxylin for 30 sec prior to dehydration and mounting.

Apoptotic cell death was assessed using a TUNEL assay with a commercially available apoptosis detection kit (ApopTag® Peroxidase In Situ Apoptosis Detection Kit; Millipore, Temecula, CA, USA) according to the manufacturer's instructions. Briefly, following routine deparaffinization, rehydration and blocking of endogenous peroxidase with 3% hydrogen peroxide in PBS for 10 min at room temperature, the tissue sections were digested with 20 $\mu$g/ml proteinase K in PBS for 15 min at room temperature. Subsequent to washing in PBS buffer, equilibration buffer was applied to the sections for 1 min at room temperature and the sections were then incubated with working strength terminal deoxynucleotidyl transferase (TdT) enzyme for 60 min at 37˚C in a humidity chamber. The reaction was terminated in Working Strength Stop/Wash buffer for 30 min at room temperature. After washing in PBS, the sections were covered with anti-digoxigenin-peroxidase for 30 min at room temperature. The color reaction was developed using DAB substrate chromogen solution for 5 min and the sections were washed with distilled water and lightly counterstained with Mayer's hematoxylin for 30 sec. All the sections were stained with hematoxylin and eosin for histological analysis.

Cell proliferation was determined by calculating the number of Ki-67-positive cell nuclei and the apoptotic cell death was determined by counting the number of TUNEL-positive cells in at least five randomly selected high-power fields (magnification, x200). Microvessel density (MVD) was also determined by calculating the number of individual microvessels stained with CD31, the endothelial cell surface marker in tumor areas without necrosis, as described in our previous study (19).

*$^1$H HR-MAS MR spectroscopy*. Prior to the $^1$H HR-MAS MRS data acquisition, the tumor samples were cut to fit a MAS rotor and flushed with deuterium oxide ($D_2O$) to remove the residual blood and water. The samples were inserted into a pre-weighed zirconium HR-MAS rotar (50 $\mu$l, 4-mm diameter) and weighed. The average tissue sample content was 7-9 mg. For chemical shift reference, TSP (3'-trimethylsilylpropionate-2,2,3,3-$d_4$) sodium salt was dissolved in $D_2O$ at a concentration of 1 mM. The remaining volume of the rotor was filled with $D_2O$ to ensure consistent spinning and each sample was transferred into the HR-MAS probe. The HR-MAS studies were conducted on a Bruker Avance 400 MHz vertical-bore spectrometer (Bruker BioSpin GmbH, Rheinstetten, Germany) equipped with a 4-mm HR-MAS $^1$H/$^{13}$C probe with a z-gradient aligned with the magic angle axis using the standard 5000 Hz spinning rate for the magnetic field strength. Spectra were obtained at 4˚C.

Two spectra were obtained for each sample, as previously described (12). A standard single-pulse spectrum (zgpr; Bruker BioSpin GmbH) with suppression of the water signal was obtained following 3 sec of water presaturation and a 60˚ flip angle over a sweep width of 20 ppm. Thereafter, a Carr-Purcell-Meiboom-Gill (CPMG) spin-echo experiment (cpmgpr; Bruker BioSpin GmbH) was performed using 2 sec of water suppression prior to a 90˚ excitation pulse. The free induction decay was collected into 64 K points during 2.72 sec, and 32 transients were collected. A total of 128 transients over a frequency region of 16.7 ppm were collected into 32 K points, resulting in an acquisition time of 1.64 sec. Spectra were Fourier-transformed into 128K after 0.3 Hz exponential line broadening. A linear baseline correction was applied, and chemical shifts were calibrated to the TSP peak at 0 ppm.

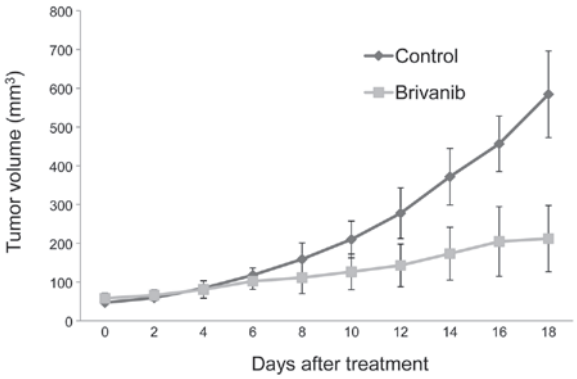


Figure 1. Inhibition of Hep3B xenograft growth by brivanib. Tumor volume curves measured using calipers in vehicle-treated control mice (n=7) and brivanib-treated mice (n=8) for 18 days. A significant reduction in tumor growth was observed for brivanib-treated mice vs. the vehicle-treated control. The mean tumor volume in the vehicle-treated mice was 584.4±111.6 mm$^3$ (mean ± SD) at the 18th day of treatment, while that in brivanib-treated mice only reached 212.2±85.5 mm$^3$ (64% reduction compared with vehicle; P<0.05).

*Statistical analysis*. Hep3B xenograft tumor volume and the HR-MAS MRS metabolite concentration were compared by the Mann-Whitney U test, and quantification of Ki-67-, CD31- and TUNEL-positive reactions were compared using the unpaired Student's t-test. P<0.05 was considered to indicate a statistically significant difference.

## Results

*In vivo tumor xenograft growth inhibition*. The antitumor activity of brivanib was investigated in a Hep3B human hepatocellular carcinoma xenograft model in athymic nude mice. Tumor growth was assessed according to tumor volume. As shown in Fig. 1, treatment with brivanib at a daily dose of 90 mg/kg body weight markedly reduced tumor growth, suggesting that brivanib is effective in xenografted Hep3B tumors. Statistically significant tumor growth inhibition was observed on the sixth day following treatment between the two groups (P<0.05). The mean tumor volume in vehicle-treated mice was 584.4±111.6 mm$^3$ (mean ± SD) on the 18th day following treatment, while that in brivanib-treated mice only reached 212.2±85.5 mm$^3$ (64% reduction compared with vehicle; P<0.05). During the study, the antitumor activity observed with brivanib treatment was not associated with any overt toxicity as judged by the lack of significant changes in body weight between the two groups (data not shown).

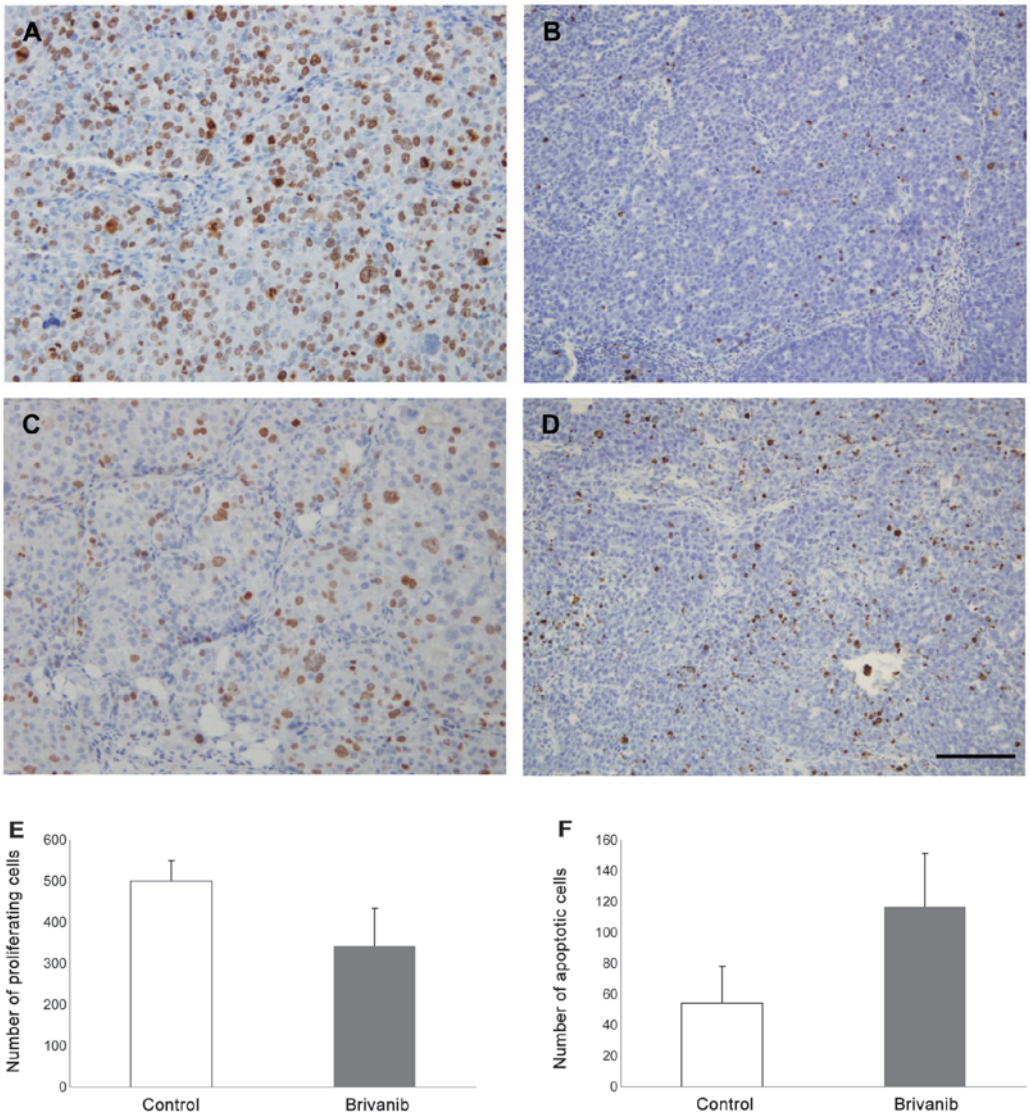


Figure 2. Effects of brivanib therapy on the proliferation and apoptosis in xenografted Hep3B tumors. Representative images of proliferation measured by immunohistochemical staining for Ki-67 (A and C) and apoptosis were analyzed by a TUNEL assay (B and D) from vehicle-treated control tumors (A and B, respectively) and brivanib-treated tumors (C and D, respectively). (E) The number of proliferating cells was determined by calculating the number of Ki-67-positive cell nuclei and (F) the number of apoptotic cells was determined by counting the number of TUNEL-positive cells in at least five randomly selected high-power fields (magnification, x200). Scale bar, 100 $\mu$m. P<0.05. TUNEL, terminal deoxynucleotidyl transferase dUTP nick end-labeling.

*Effects on cell proliferation and apoptosis*. Based on the results with regard to *in vivo* tumor growth inhibition, the anti-proliferative effects of brivanib at the cell level were assessed by quantifying tumor cell proliferation measured by immunohistochemical staining for Ki-67 and apoptosis analyzed by a TUNEL assay 18 days following treatment, as described in Materials and methods. Quantitative analysis was performed on a total of 15 mice (n=7 control and n=8 treated). As expected, the mean number of Ki-67-positive tumor cells was substantially decreased, while the mean number of TUNEL-positive cells, which was inversely related to Ki-67-positivity, was significantly increased in brivanib-treated tumor cells (Fig. 2A-D). As shown in Fig. 2E and F, the mean number of Ki-67-positive tumor cells (proliferating cells) in vehicle-treated mice was 499.33±50.05, but that in brivanib-treated mice was 341.51±92.32 (32% reduction compared with vehicle; P<0.05), while the mean number of TUNEL-positive cells (apoptotic cells) was 54.20±23.76 in vehicle-treated mice and 116.53±34.67 (54% increase compared with vehicle; P<0.05) in brivanib-treated mice. These observations suggested that the antitumor activity of brivanib in Hep3B xenografts may be attributed to the inhibition of cell proliferation and the induction of apoptotic cell death.

*Effect on MVD*. The specific effects of brivanib on tumor microvasculature from vehicle-treated and brivanib-treated animals were immunohistochemically analyzed with CD31 antibody reactivity in vascular tumor areas without necrosis. As shown in Fig. 3, tumor microvessels were significantly reduced in tumor tissue from brivanib-treated mice compared with tumor tissue from vehicle-treated mice. MVD in vehicle-treated mice was 58.51±13.37 18 days following treatment, but that in brivanib-treated mice was 28.42±8.26. There was a significant reduction in brivanib-treated tumor MVD compared with the vehicle-treated tumor (51% reduction; P<0.05). These results are consistent with the hypothesis that targeting tumor-associated

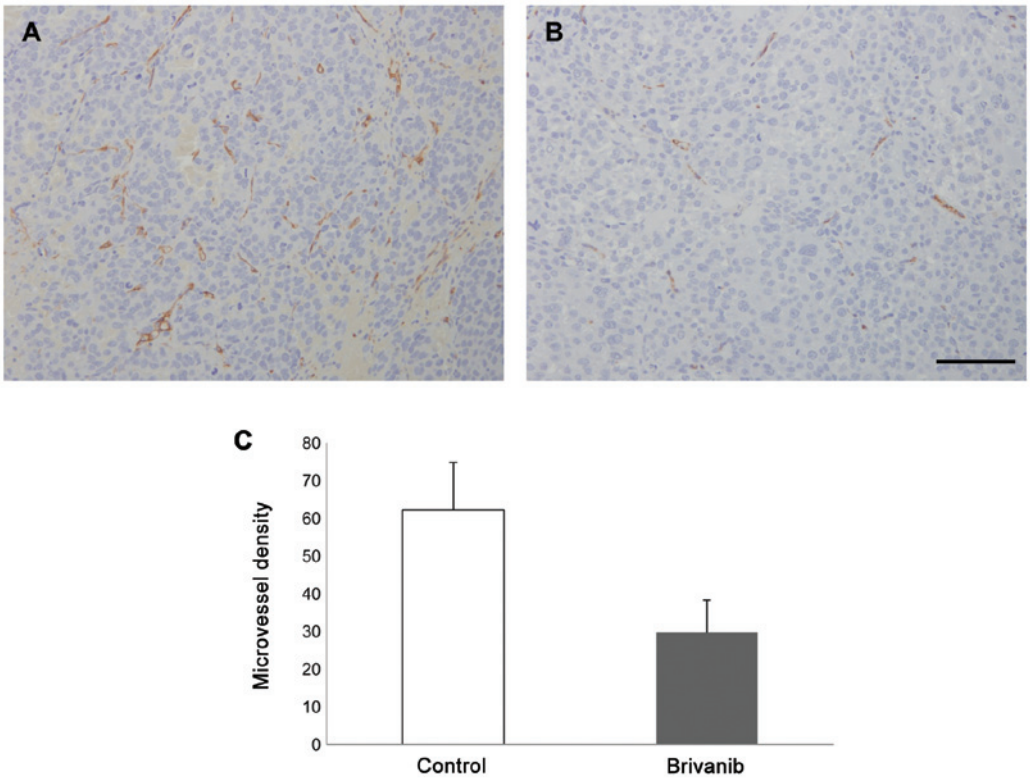


Figure 3. Effects of brivanib therapy on the microvasculature in xenografted Hep3B tumor. Representative images of immunohistochemistry staining for the CD31 antibody in (A) vehicle-treated control tumors and (B) brivanib-treated tumors. Vessels are stained dark brown. (C) Microvessel density was determined by calculating the number of individual microvessels stained with CD31 in at least five randomly selected high-power fields (magnification, x200). Scale bar, 100 $\mu$m. P<0.05.

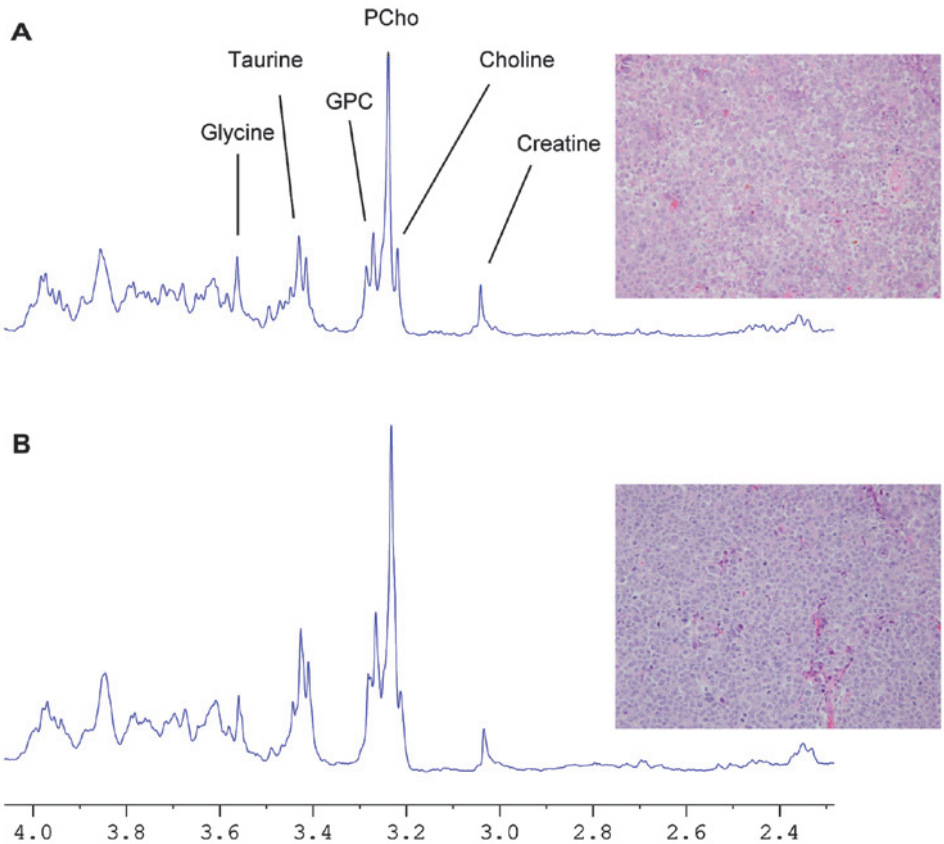


Figure 4. Representative $^{1}$H high-resolution magic angle spinning magnetic resonance spectroscopy and corresponding histopathologic sections from (A) brivanib-treated and (B) vehicle-treated control Hep3B tumor xenografts. Spectral assignments are provided for peak area calculations to estimate tissue concentrations of the selected predominant metabolites in the spectral region 3.6-3.0 ppm. GPC, glycerophosphocholine; PCho, phosphocholine.

angiogenesis is a primary mechanism of antitumor activity of brivanib in the Hep3B xenograft model.

*$^{1}$H HR-MAS MR spectroscopy*. To investigate the effect of brivanib treatment on xenografted Hep3B tumor metabolism, $^{1}$H HR-MAS MRS was used as described in Materials and methods. Representative $^{1}$H HR-MAS spectra from a control and a treated tumor are shown in Fig. 4 with assignments for the majority of the metabolites, including glycine (3.56 ppm), taurine (3.42 ppm), glycerophosphocholine (GPC, 3.23 ppm), phosphocholine (PCho, 3.21 ppm), choline (Cho, 3.19 ppm) and creatine (3.04 ppm). As shown in the results, the HR-MAS MRS analyses demonstrated significant differences in the choline-containing metabolic profiles (Cho, PCho and GPC) between vehicle-treated control mice (n=7) and brivanib-treated mice (n=8). The choline-containing metabolites tended to decrease in brivanib-treated tumor tissues. The concentration of PCho, which was the largest peak in the two groups was 6.56±1.28 $\mu$mol/g in the vehicle-treated control mice and 5.54±0.97 $\mu$mol/g in the brivanib-treated mice, while the concentration of GPC was 3.49±0.82 $\mu$mol/g in the vehicle-treated control mice and 2.45±0.18 $\mu$mol/g in the brivanib-treated mice ($P<0.05$, Mann-Whitney U test).

## Discussion

In the present study, $^{1}$H HR-MAS and histopathology were used to investigate the effects of treatment with brivanib in a human HCC xenograft. As shown in the results, brivanib, a novel, dual tyrosine kinase inhibitor with selectivity against VEGF and FGF receptors, effectively inhibited tumor growth in Hep3B xenografts and was associated with the inhibition of angiogenesis, increased apoptosis and inhibition of cell proliferation.

Generally, HCC tumors are hypervascularized, suggesting that they may be particularly vulnerable to angiogenesis inhibition (20). Several endogenous proangiogenic factors and modulators are expressed in HCC, and studies have indicated that they may be involved in HCC pathogenesis. A number of studies have indicated that VEGF and basic FGF are important proangiogenic factors that are central in the progression of HCC by promoting tumor angiogenesis and subsequent growth and metastasis (21,22). VEGF is considered to be one of the most important angiogenic factors involved in HCC vascularization. Elevated expression of VEGF is associated with histopathologic tumor grade, postoperative recurrence, poor prognosis and tumor microvessel density in HCC (23). Overexpression of bFGF is also detected in patients with HCC. Basic FGF stimulates the release and activity of collagenases, proteases and integrins on the extracellular membrane to form nascent microvascular networks. Furthermore, bFGF has been shown to synergistically increase VEGF-mediated HCC development and angiogenesis (24,25). Due to the complex interactions among tumor cells, the invading stroma and novel blood vessels, therapeutic antiangiogenic agents that target a single angiogenic molecule have shown limited efficacy in clinical trials (26,27). Thus, the dual inhibition of VEGF and FGF signaling pathways, which promote angiogenesis and metastasis may be a novel antiangiogenic therapeutic strategy in HCC. Therefore, brivanib, a dual inhibitor of VEGFR and FGFR tyrosine kinases was administered in an HCC xenograft model in the present study.

In several tumor xenograft models, the daily administration of brivanib induced significant tumor growth inhibition. Brivanib has shown significant dose-dependent tumor growth inhibition in breast, colon and lung xenograft models (11). However, the exact mechanisms by which brivanib treatment induces growth inhibition are not well understood. Brivanib may prevent the tumor mass from expanding by disrupting the supply of nutrients and growth factors to the tumor cells. In addition, results of previous *in vitro* and *in vivo* studies have shown that brivanib affects the host endothelium (9,11). In a preclinical study, brivanib significantly suppressed tumor growth in six HCC xenograft lines when orally administered once daily (10). Consistent with results from other studies, the results of the present study have demonstrated that the daily administration of brivanib significantly inhibited the growth of Hep3B xenografts. Brivanib therapy decreased tumor growth by 64%. Immunohistochemical analyses demonstrated that treatment with brivanib exhibited a significant effect on the inhibition of cell proliferation and induction of apoptosis in tumors compared with the vehicle-treated control, suggesting that brivanib results in apoptosis of the Hep3B xenograft tumor. The results of the present study also showed that the marked reduction in MVD with brivanib therapy compared with vehicle-treated control is noteworthy, as a decrease in tumor vessel density induced by antiangiogenic agents is expected to reduce tumor perfusion and thereby oxygen delivery. The balance between the proangiogenic and antiangiogenic molecules released by tumor cells and surrounding host cells determines the intense tumor vascularization. Previous studies have demonstrated that VEGF-positive tissue was associated with a high MVD expression, whereas VEGF-negative tissue demonstrated a low expression of MVD, suggesting a positive correlation between VEGF and MVD (28). This result suggests that the potent antiangiogenic activity of brivanib is the primary mechanism of the inhibition of tumor growth in a Hep3B xenograft animal model.

A number of HR-MAS MRS approaches have demonstrated altered tumor metabolic profiles for treated tumors, in conjunction with subsequent histopathology of the same tumor specimen, which supports histopathological examination and improves the accuracy in the diagnosis, characterization, and evaluation of tumor progression in different tumors (12,16,17). In this study, $^{1}$H HR-MAS MRS was used to investigate how brivanib treatment influences the metabolic profiles of Hep3B xenografts. As shown in the results, the $^{1}$H HR-MAS MR spectra were dominated by choline, creatine and taurine in the region above 3 ppm. The $^{1}$H HR-MAS spectra show significantly higher levels of PCho and GPC in the vehicle-treated control tumors, supporting the hypothesis that brivanib treatment induces changes in metabolism. It has been previously observed that the choline metabolites that are regulated by several signaling pathways are important in phospholipid metabolism and these choline metabolites increase with tumor malignancy (29,30). The *in vivo* choline metabolite signal is dependent upon the cellular concentrations of GPC, PCho and Cho. Several biochemical studies have suggested that PCho is a precursor as well as a breakdown product of the predominant membrane component phosphatidylcholine, whereas GPC is

solely a membrane breakdown product (31). In accordance with previous studies, the decreased choline-containing metabolites as a therapeutic response to brivanib in the present $^{1}$H HR-MAS MRS results may be due to decreased cell density, which is in agreement with histopathology showing decreased cell proliferation and increased apoptotic cell death.

In conclusion, this study has shown that the vascular targeting agent brivanib is highly efficacious in Hep3B xenograft and is associated with an inhibition of angiogenesis, increased apoptosis and inhibition of cell proliferation. Furthermore, the results suggested that the additional information obtained by HR-MAS MRS metabolic profiling may be a feasible tool for evaluating the therapeutic response and supporting histopathological analysis through the quantification of altered metabolic profiles following treatment with therapeutic agents.

## Acknowledgements

This study was conducted with the support of a grant (to D.I.C.) from the Korean Healthcare Technology R&D Project, Ministry for Health, Welfare and Family Affairs, Korea (grant no: A102142).

## References

1. Folkman J: What is the evidence that tumors are angiogenesis dependent? J Natl Cancer Inst 82: 4-6, 1990.
2. Ferrara N: Vascular endothelial growth factor as a target for anticancer therapy. Oncologist 9 (Suppl 1): 2-10, 2004.
3. Hicklin DJ and Ellis LM: Role of the vascular endothelial growth factor pathway in tumor growth and angiogenesis. J Clin Oncol 23: 1011-1027, 2005.
4. Kerbel RS: Tumor angiogenesis. N Engl J Med 358: 2039-2049, 2008.
5. Presta M, Dell'Era P, Mitola S, Moroni E, Ronca R and Rusnati M: Fibroblast growth factor/fibroblast growth factor receptor system in angiogenesis. Cytokine Growth Factor Rev 16: 159-178, 2005.
6. Turner N and Grose R: Fibroblast growth factor signalling: from development to cancer. Nat Rev Cancer 10: 116-129, 2010.
7. Hurwitz H, Fehrenbacher L, Novotny W, Cartwright T, Hainsworth J, Heim W, Berlin J, Baron A, Griffing S, Holmgren E, Ferrara N, Fyfe G, Rogers B, Ross R and Kabbinavar F: Bevacizumab plus irinotecan, fluorouracil, and leucovorin for metastatic colorectal cancer. N Engl J Med 350: 2335-2342, 2004.
8. Cheng AL, Kang YK, Chen Z, Tsao CJ, Qin S, Kim JS, Luo R, Feng J, Ye S, Yang TS, *et al*: Efficacy and safety of sorafenib in patients in the Asia-Pacific region with advanced hepatocellular carcinoma: a phase III randomised, double-blind, placebo-controlled trial. Lancet Oncol 10: 25-34, 2009.
9. Diaz-Padilla I and Siu LL: Brivanib alaninate for cancer. Expert Opin Investig Drugs 20: 577-586, 2011.
10. Huynh H, Ngo VC, Fargnoli J, Ayers M, Soo KC, Koong HN, Thng CH, Ong HS, Chung A, Chow P, Pollock P, Byron S and Tran E: Brivanib alaninate, a dual inhibitor of vascular endothelial growth factor receptor and fibroblast growth factor receptor tyrosine kinases, induces growth inhibition in mouse models of human hepatocellular carcinoma. Clin Cancer Res 14: 6146-6153, 2008.
11. Marathe PH, Kamath AV, Zhang Y, D'Arienzo C, Bhide R and Fargnoli J: Preclinical pharmacokinetics and in vitro metabolism of brivanib (BMS-540215), a potent VEGFR2 inhibitor and its alanine ester prodrug brivanib alaninate. Cancer Chemother Pharmacol 65: 55-66, 2009.
12. Sitter B, Lundgren S, Bathen TF, Halgunset J, Fjosne HE and Gribbestad IS: Comparison of HR MAS MR spectroscopic profiles of breast cancer tissue with clinical parameters. NMR Biomed 19: 30-40, 2006.
13. Beckonert O, Coen M, Keun HC, Wang Y, Ebbels TM, Holmes E, Lindon JC and Nicholson JK: High-resolution magic-angle-spinning NMR spectroscopy for metabolic profiling of intact tissues. Nat Protoc 5: 1019-1032, 2010.
14. Cheng LL, Burns MA, Taylor JL, He W, Halpern EF, McDougal WS and Wu CL: Metabolic characterization of human prostate cancer with tissue magnetic resonance spectroscopy. Cancer Res 65: 3030-3034, 2005.
15. Swanson MG, Zektzer AS, Tabatabai ZL, Simko J, Jarso S, Keshari KR, Schmitt L, Carroll PR, Shinohara K, Vigneron DB and Kurhanewicz J: Quantitative analysis of prostate metabolites using $^{1}$H HR-MAS spectroscopy. Magn Reson Med 55: 1257-1264, 2006.
16. Erb G, Elbayed K, Piotto M, Raya J, Neuville A, Mohr M, Maitrot D, Kehrli P and Namer IJ: Toward improved grading of malignancy in oligodendrogliomas using metabolomics. Magn Reson Med 59: 959-965, 2008.
17. Rocha CM, Barros AS, Gil AM, Goodfellow BJ, Humpfer E, Spraul M, Carreira IM, Melo JB, Bernardo J, Gomes A, Sousa V, Carvalho L and Duarte IF: Metabolic profiling of human lung cancer tissue by $^{1}$H high resolution magic angle spinning (HRMAS) NMR spectroscopy. J Proteome Res 9: 319-332, 2010.
18. Sitter B, Bathen T, Hagen B, Arentz C, Skjeldestad FE and Gribbestad IS: Cervical cancer tissue characterized by high-resolution magic angle spinning MR spectroscopy. MAGMA 16: 174-181, 2004.
19. Yang J, Kim JH, Im GH, Heo H, Yoon S, Lee J, Lee JH and Jeon P: Evaluation of antiangiogenic effects of a new synthetic candidate drug KR-31831 on xenografted ovarian carcinoma using dynamic contrast enhanced MRI. Korean J Radiol 12: 602-610, 2011.
20. Frenette C and Gish R: Targeted systemic therapies for hepatocellular carcinoma: clinical perspectives, challenges and implications. World J Gastroenterol 18: 498-506, 2012.
21. Miura H, Miyazaki T, Kuroda M, Oka T, Machinami R, Kodama T, Shibuya M, Makuuchi M, Yazaki Y and Ohnishi S: Increased expression of vascular endothelial growth factor in human hepatocellular carcinoma. J Hepatol 27: 854-861, 1997.
22. Torimura T, Sata M, Ueno T, Kin M, Tsuji R, Suzaku K, Hashimoto O, Sugawara H and Tanikawa K: Increased expression of vascular endothelial growth factor is associated with tumor progression in hepatocellular carcinoma. Hum Pathol 29: 986-991, 1998.
23. Moon WS, Rhyu KH, Kang MJ, Lee DG, Yu HC, Yeum JH, Koh GY and Tarnawski AS: Overexpression of VEGF and angiopoietin 2: a key to high vascularity of hepatocellular carcinoma? Mod Pathol 16: 552-557, 2003.
24. Hsu PI, Chow NH, Lai KH, Yang HB, Chan SH, Lin XZ, Cheng JS, Huang JS, Ger LP, Huang SM, Yen MY and Yang YF: Implications of serum basic fibroblast growth factor levels in chronic liver diseases and hepatocellular carcinoma. Anticancer Res 17: 2803-2809, 1997.
25. Mise M, Arii S, Higashituji H, Furutani M, Niwano M, Harada T, Ishigami S, Toda Y, Nakayama H, Fukumoto M, Fujita J and Imamura M: Clinical significance of vascular endothelial growth factor and basic fibroblast growth factor gene expression in liver tumor. Hepatology 23: 455-464, 1996.
26. Adams J, Huang P and Patrick D: A strategy for the design of multiplex inhibitors for kinase-mediated signalling in angiogenesis. Curr Opin Chem Biol 6: 486-492, 2002.
27. Laird AD and Cherrington JM: Small molecule tyrosine kinase inhibitors: clinical development of anticancer agents. Expert Opin Investig Drugs 12: 51-64, 2003.
28. Li W, Liu ML, Cai JH, Tang YX, Zhai LY and Zhang J: Effect of the combination of a cyclooxygenase-1 selective inhibitor and taxol on proliferation, apoptosis and angiogenesis of ovarian cancer *in vivo*. Oncol Lett 4: 168-174, 2012.
29. Jensen LR, Huuse EM, Bathen TF, Goa PE, Bofin AM, Pedersen TB, Lundgren S and Gribbestad IS: Assessment of early docetaxel response in an experimental model of human breast cancer using DCE-MRI, ex vivo HR MAS, and in vivo $^{1}$H MRS. NMR Biomed 23: 56-65, 2010.
30. Moestue S, Sitter B, Bathen TF, Tessem MB and Gribbestad IS: HR MAS MR spectroscopy in metabolic characterization of cancer. Curr Top Med Chem 11: 2-26, 2011.
31. Seierstad T, Røe K, Sitter B, Halgunset J, Flatmark K, Ree AH, Olsen DR, Gribbestad IS and Bathen TF: Principal component analysis for the comparison of metabolic profiles from human rectal cancer biopsies and colorectal xenografts using high-resolution magic angle spinning $^{1}$H magnetic resonance spectroscopy. Mol Cancer 7: 33, 2008.